Sustainable Futures 4 (2022) 100093

Contents lists available at ScienceDirect

Sustainable Futures

journal homepage: www.sciencedirect.com/journal/sustainable-futures

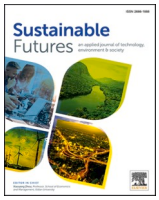

"Re-engineering of a food oven for thermal sanitization of Personal Protective Equipment against Sars-CoV-2 virus"

Eleonora Bottani [a], Benedetta Bottari [b], Daniel Milanese [a], Roberto Montanari [a], Corrado Sciancalepore [a], Andrea Volpi [a,*], Federico Solari [a], Letizia Tebaldi [a]

[a] Department of Engineering and Architecture, University of Parma, Parco Area delle Scienze 181/A, Parma 43124, Italy
[b] Department of Food and Drug, University of Parma, Parco Area delle Scienze 49/A, Parma 43124, Italy

ARTICLE INFO

Keywords:
Thermal sanitization
Thermal process
Heat process
Personal Protective Equipment
COVID-19 pandemic
CFD simulation
Biological risk

ABSTRACT

One of the main issues addressed by the recent COVID-19 pandemic which affected the whole world is the availability of Personal Protective Equipment (PPE) (e.g., face masks, white coats, or disposable gloves). This issue impacts on sustainability from different perspectives, such as more generated waste or environmental pollution, both for manufacturing and disposal, or more inequalities deriving from who can afford and access PPE and who cannot, since many shortages were recorded during the pandemic as well as fluctuating unit prices. Moreover, quite often PPE intended for single use are improperly used more times, thus generating a biological risk of infection. In an attempt to propose an innovative solution to face this problem, in this paper the re-design of an oven originally intended for food purposes is presented, with the aim of operating a thermal sanitization of PPE. The machinery and its components are detailed, together with physical and microbiological tests performed on non-woven PPE to assess the effect of treatment on mechanical properties and viral load. The pilot machinery turned out to be effective in destroying a bovine coronavirus at 95 °C and thus reducing contaminating risk in one hour without compromising the main properties of PPE, opening perspectives for the commercialization of the solution in the near future.

1. Introduction

Year 2020 will surely go down in history as the COVID-19 pandemic year, which has triggered millions of deaths around the world. Several problems arose, being health, medical, but also industrial and environmental related. Indeed, among the main issues addressed, for sure the topic of Personal Protective Equipment (PPE) deserves attention. For health PPE it is meant an effective control measure occurring when exposures to pathogens cannot be eliminated [1], thus posing a health risk; examples of PPE are face masks, disposable gloves, white coats or goggles. Two main problems emerged related to this topic: first of all, the shortage of equipment, and secondly (and consequently), their inappropriate usage, which quite often results in items intended for single use being reused or worn for longer periods than recommended [2].

If we think that the demand for PPE is not expected to decline during the post-pandemic period, but is rather estimated to increase 20% up to 2025 [3], it follows that some actions and strategies may be developed and adopted, in order to face a continuous and growing demand, with subsequent consequences which could be involved (e.g. repeated eventual shortages, increase in waste or in spending from private individuals but also companies which must be able to guarantee PPE for their workers).

Strategies of PPE sanitisation are already present in the literature, such as via radiation, or by chemical and thermal treatment. Some of them, e.g. Gamma and UV rays were shown to compromise the filtering capacity when tested on face masks, while not being able to decontaminate treated PPE (e.g., [4,5]). Hydrogen peroxide was frequently used without affecting the filtering capacity of PPE (e.g., [6,7]), and was recently successfully applied also on Sars-Cov-2 virus [8], even if the authors provided just some preliminary outcomes. Ozone as well can be involved for sterilisation purposes, showing good performances on Sars-Cov-2 under high relative humidity conditions [9]. In addition, alcoholic solutions can be applied through immersion or superficial spraying [10], even if the first case results in a decrease of the filtering capacity, and the second has a limited durability (its usage is

* Corresponding author.
E-mail address: andrea.volpi@unipr.it (A. Volpi).

https://doi.org/10.1016/j.sftr.2022.100093
Received 14 April 2022; Received in revised form 8 July 2022; Accepted 9 August 2022
Available online 12 August 2022

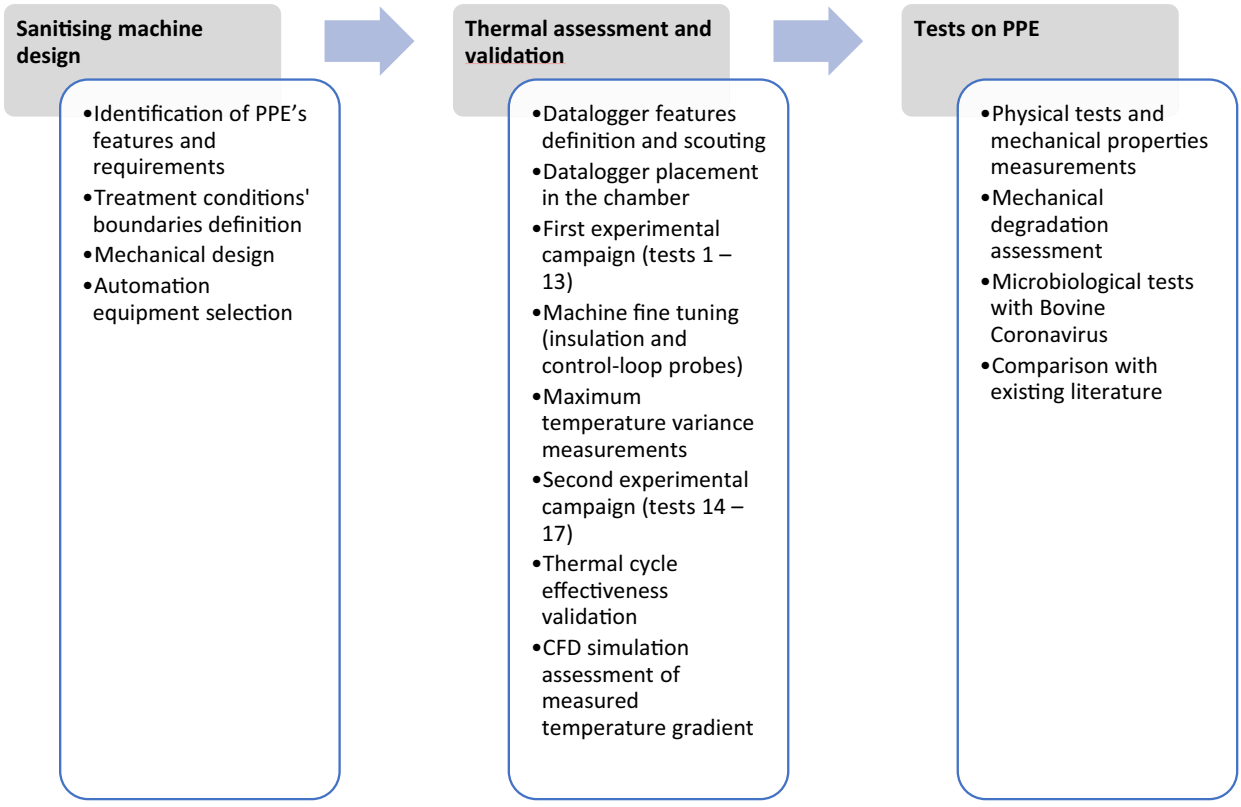

Fig. 1. (a) Methodological approach of the study. (b) The machine for thermal PPE disinfection (3D view on the left, real machinery on the right).

comparable with that of hand sanitizing gel).

Little evidence of thermal treatments on the Sars-CoV-2 virus for PPE sanitisation emerged from literature, surely due to the novelty of the topic, and no solutions intended to be industrialised and commercialised are already available.

According to these short premises, the present study aims at proposing a possible solution to face the above-mentioned problems under a sustainability perspective and at the same time at reducing the biological risk for users. Specifically, a machine for the thermal sanitisation of disposable PPE starting from a simple food oven was designed at the Department of Engineering and Architecture of the University of Parma (Italy) together with a company producing machinery for the food industry based in the north of Italy, namely Nilma S.p.A. (https://nilma.com/eng). The *SAFER 10 Lavacamici* (meaning "white coats washer" in Italian) allows disposable devices to be reused, thus reducing unnecessary waste, allowing economic savings and reducing the demand for new PPE under safety conditions.

Overall, the purpose of the study is to address the two following Research Questions (RQ):

RQ1: Which are the requirements of a thermal cycle able to sanitize from Sars-CoV-2 disposable non-woven fabrics PPE, thus reducing the risk of contamination?

RQ2: Is it possible, from the perspective of a food machinery manufacturing company, to provide an industrial solution to be commercialised for thermal sanitizing of PPE?

The manuscript is structured as follows: Section 2 illustrates the project phases and methodology; in Section 3 the machine and the different tests are proposed, followed by a discussion section (Section 4); finally, Section 5 concludes the manuscript with a resume of the work done, its implications as well as possible future actions.

2. Methodology and project phases

In this section the methodology followed and the steps constituting the project are briefly introduced.

The methodological approach folllowed for providing proper answers to the presented research questions is depicted in Fig. 1.

The design of the machine begins with a brief literature analysis, carried out to investigate the existence of thermal treatments on available PPE for Sars-CoV-2 virus and, eventually, to study their requirements in terms of duration and temperature for selecting the combination to be involved in the testing phase of the present study and make comparisons. Concurrently, the selection of the proper oven model to be converted into a thermal sanitizer was performed together with Nilma's management. Once equipped with the required automation tools and equipment, including removable temperature dataloggers, the machine was validated through 17 laboratory testing sessions; specifically, these tests also allowed to refine the machinery configuration step by step and were preparatory to the solution fine tuning, assessing the maximum temperature variance. Moreover, to confirm the experimental measurements, a Computational Fluid Dynamics (CFD) simulation was performed to determine the temperature distribution within the chamber; this part of the research was previously presented in Bottani et al. [11].

After validation, physical tests were performed on some selected PPE (non-woven fabric disposable white coats and face masks) for assessing the material behaviour after the thermal treatment and its mechanical properties. Finally, microbiological tests were performed on the same PPE inoculated with Bovine Coronavirus (BCoV) to investigate the ability of the treatment in reducing the viral load, comparing the obtained results with those available in literature.

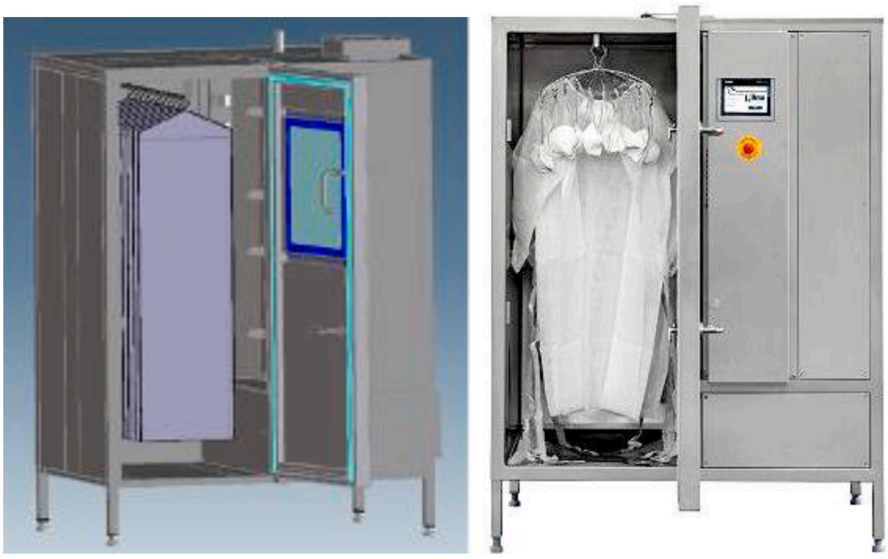

Fig. 2. The machine for thermal PPE disinfection (3D view on the left, real machinery on the right).

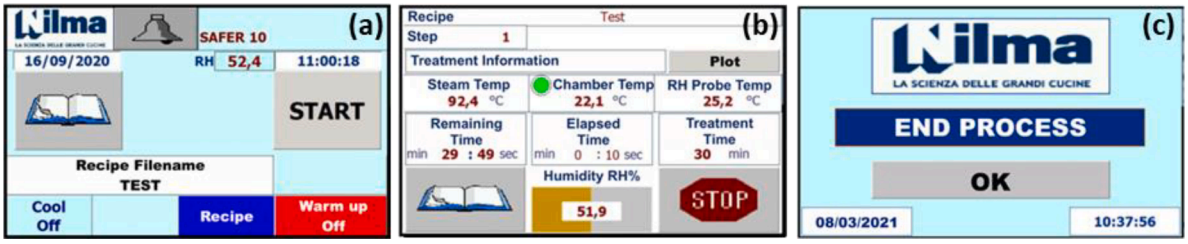

Fig. 3. Human-machine interface (HMI). (**a**) Initial interface; (**b**) interface while the machine is running; (**c**) ending interface.

3. Results

3.1. Machinery design, thermal assessment and validation

The developed machinery is entirely made of stainless steel and is designed to host up to 11 white coats, properly distanced among them and the insides (13 cm between white coats and walls are guaranteed, and 10 cm from the base). White coats, with an estimated average length of 1400 mm, are placed for treatment on hangers measuring 410 × 180 mm^2, made of stainless steel as well, with a 2.5 mm thickness. The size of the selected chamber is 1,693 × 1,010 × 670 mm^3 (model KS40XP designed by Nilma S.p.A.). Hygienic design criteria were properly adopted in the development. The machinery (shown in Fig. 2) is equipped with:

- relative humidity sensor, able to assess the different saturation level within the chamber.
- double temperature sensor to monitor the temperature of the outlet air produced by the heater (Probe 1) and of the PPE (Probe 2).
- electric steam generator (relative pressure set at 0.2 bar, safety valve at 0.5 bar), including resistors as the chamber is supposed to work in a dry environment.
- fans system, able of processing a 2,256 m^3/h flow rate.
- a touch control panel for easily letting the operators interact with it and set the desired parameters (temperature, humidity and treatment duration); its interface is shown in Fig. 3.

The machine automation is based on a couple of closed-loop controllers. The first manages the chamber temperature according to the desired set point and can rely on Probe 1 (a PT100 sensor installed on the heater air outlet) or on Probe 2 (a combined temperature and relative humidity sensor positioned on the top area A of the chamber). The second controls the steam generator according to the chamber humidity measured by Probe 2.

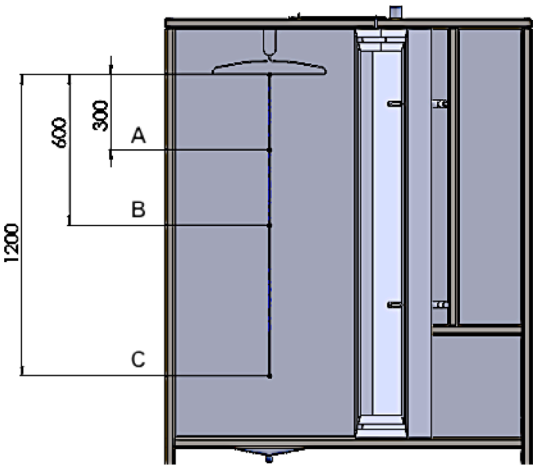

Fig. 4. Chamber volume subdivision.

Once the chamber has been designed, a proper validation campaign was required, both to check the functioning of the machine and to assess its thermal behaviour.

To carry out these tests, the volume of the chamber was split into three bands referring to position A (top), B (centre) and C (bottom), which were then used as a reference as shown in Fig. 4. The sensors, arranged on the white coats, were uniformly distributed across one or

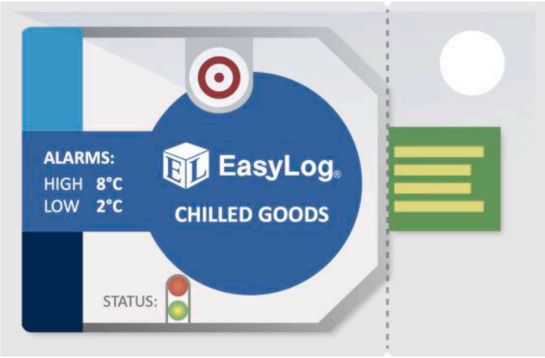

Fig. 5. EasyLog Cold Chain sensor.

more of these bands according to a pre-established mapping scheme developed for the specific test ID.

To map the temperature distribution, 15 EasyLog CC data loggers manufactured by Lascar Electronics were selected (Fig. 5), chosen for their flexibility, accuracy, and overall cost/performance trade-off. Indeed, these data loggers can be used in various contexts, and perfectly match the requirements of the studied system, namely: logging capability for long period (32,600 readings), long-lasting battery, minimum sampling interval of 1 min, small size, no need for cables, suitable temperature range. Despite their low purchasing cost, the accuracy of the probe in our range is ±0.5 °C. However, the technical sheet (Fig. 6) reports a maximum measurable temperature of +60 °C while, in the present application, +95 °C were needed. This limitation is imputable to the battery equipping the logger and not to the temperature sensor itself (a HTU21D I2C sensor IC), which is actually capable of measuring up to +125 °C. To overcome this limitation, lithium sensor batteries have been preventively replaced with extended-temperature CR2032 batteries enduring up to +95 °C (Fig. 7).

During the test campaign, the 15 data loggers were positioned into the chamber according to the test ID (shown in Table 1): they can be uniformly distributed in the whole volume of the 3 bands (configuration A-B-C) or mostly concentrated in a specific band under investigation (configuration A for assessing temperatures in the top band, B for centre, C for bottom). Data loggers were fixed by means of a tensioning and damping system consisting of springs installed on the hangers, which are tied by cables to metal rods at the bottom as depicted in Fig. 8, where specifically the A-B-C configuration is considered for monitoring the whole chamber. Fig. 9, instead, shows the two already mentioned probes' positions.

Table 1 summarizes the main data obtained in the 17 experiments performed. It is divided into two sections: the first one (tests 1 to 13) reports data obtained during experimental campaigns aimed at supporting the design of the machine, while the second one (tests 14 to 17) shows data for validating the thermal cycles on white coats. Note that for these last four tests only the chamber was full of white coats in each position (accordingly, 11 in total); otherwise, it was left empty, as the main goal was simply to map the temperature gradient inside the chamber. As far as the insulation is concerned, if no tick is present the chamber was not insulated at all; one tick (√) refers to insulation only on the side walls and two ticks (√√) mean full insulation.

As already stated, the first series of tests aimed at evaluating the behaviour of the machine in different working conditions to properly refine it. The following list details the specific functionality of each group of tests.

- Tests 1 to 4 confirmed that the adoption of a steam generator guarantees a uniform heat distribution inside the chamber (the maximum variance is approximately 1 °C). The set point is respected quite precisely although the feedback probe is not in the optimal position (it is placed on the heat air outlet and not directly in the chamber); no insulation was installed in these cases. Different bands (A, B, C) have minimal differences, thanks to the steam heat exchange ability. The steady state condition requires long time to be reached, thus suggesting the need for insulating the side walls in the following test sessions.
- Tests 5 and 6 compared the behaviour of the machine under steam and dry conditions: as expected, the higher convective properties of steam helped to mitigate the differences in temperatures.
- Tests 7 and 8 pointed out, under dry heat condition, the temperature gradient due to height; the set point is much more difficult to follow in zone C (bottom) rather than zone A (top).
- Test 9 was aimed at replicating test 8 with some improvements in the machine setting: insulation was installed also on the bottom floor of the chamber and probe 2 (placed inside the chamber) was used to close the control loop of the temperature. Unfortunately, probe 2 was faulty and, after 20 min, the test was interrupted as temperature was uncontrollably rising: more than 92 °C were reached in the chamber.
- Tests 10 and 11 compared the temperature closed control loop behaviour under dry heat conditions and according to the feedback

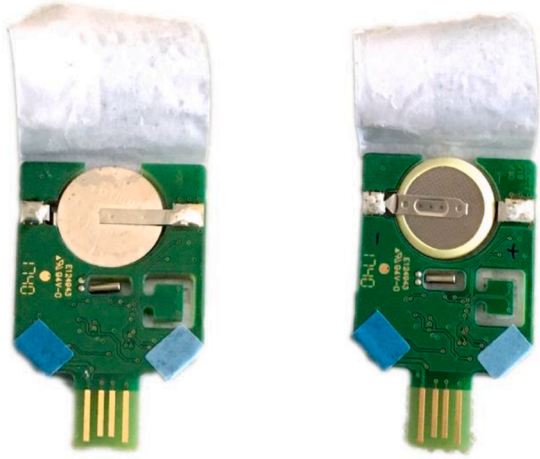

Fig. 7. Sensors equipped with CR2032 batteries: standard (left) and extended-temperature (right).

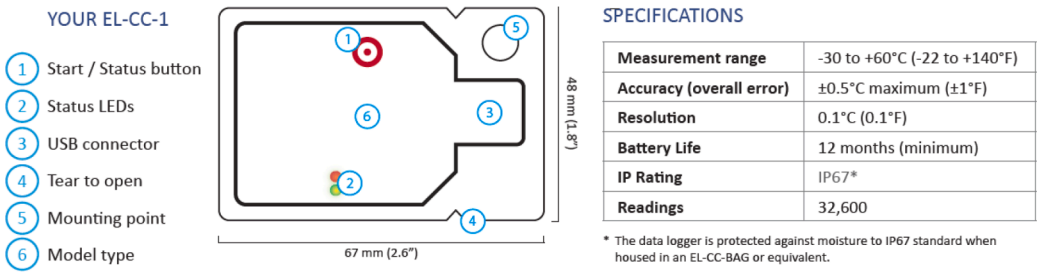

Fig. 6. EasyLog Cold Chain sensor specifications sheet.

Table 1
Characteristics and main results from the 17 tests carried out to validate the machine.

Test ID	Heat	Insulation	Loop	White Coats	Logger Position	Cycle duration [min]	Set Point [°C]	Average Temperature [°C]	Max Temperature [°C]	Max variance [°C] at end time
1	Steam	-	Probe 1		A-B-C	60	75	74.5	74.9	0.9
2	Steam	-	Probe 1		A	60	75	74.6	74.9	0.4
3	Steam	-	Probe 1		B	60	75	74.5	74.9	0.9
4	Steam	-	Probe 1		C	60	75	74.3	74.8	1.1
5	Dry	√	Probe 1		A-B-C	60	75	66.1	69.3	5.8
6	Steam	√	Probe 1		A-B-C	60	75	74.5	75.1	0.9
7	Dry	√	Probe 1		A	60	75	68.4	71.7	9.2
8	Dry	√	Probe 1		C	60	75	65.2	68.0	5.6
9	Dry	√√	Probe 2		C	20*	75	79.5	92.8	19.6
10	Dry	√√	Probe 1		A-B-C	60	75	66.3	69.2	5.3
11	Dry	√√	Probe 2		A-B-C	60	75	75.1	78.5	10.7
12	Dry	√√	Probe 2		A-B-C	60	75	77.3	81.6	7.0
13	Steam	√√	Probe 2		A-B-C	60	75	76.9	81.1	3.5
14	Steam	√√	Probe 2	√	A-B-C	60	85	83.7	88.2	6.1
15	Dry	√√	Probe 2	√	A-B-C	120	85	84.3	90.2	10.5
16	Steam	√√	Probe 2	√	A-B-C	60	95	93.4	97.4	8.1
17	Steam	√√	Probe 2	√	A-B-C	120	95	94.1	95.5	6.3

*fault in probe 2.

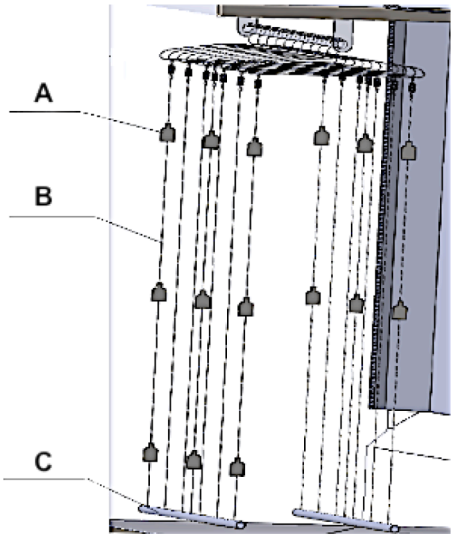

Fig. 8. Supports for positioning the 15 data loggers.

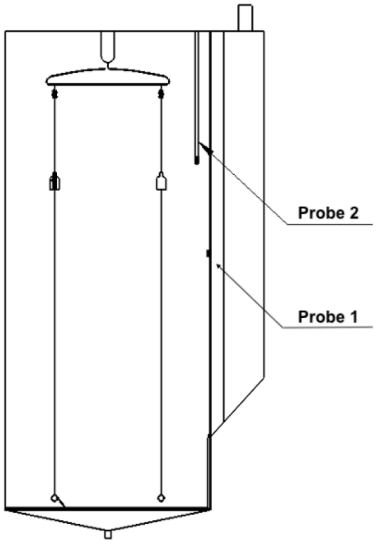

Fig. 9. Probes' position within the chamber.

taken from probe 1 or probe 2 (replaced with a new working one). Probe 2 guarantees a more precise respect of the set point but shows a higher temperature variance: this behaviour can be reasonably understood considering that the duration of heating transient was much shorter and thus presenting higher unevenness.

- Test 12 replicated test 11, and specifically it was an attempt to start a heat cycle on a warm machine instead of waiting for the machine to cool down. As expected, performances were better in this case.
- Test 13 replicated test 11, using steam instead of dry heat.

According to the above results, the company decided to keep the machine fully insulated, use the steam generator and feedback the control loop on the temperature signal of probe 2. However, probe 1 was still used to monitor the temperature trend and to perform an emergency shutdown of the machine in case it rises above 105 °C.

The second series of tests aimed at validating the effectiveness of the

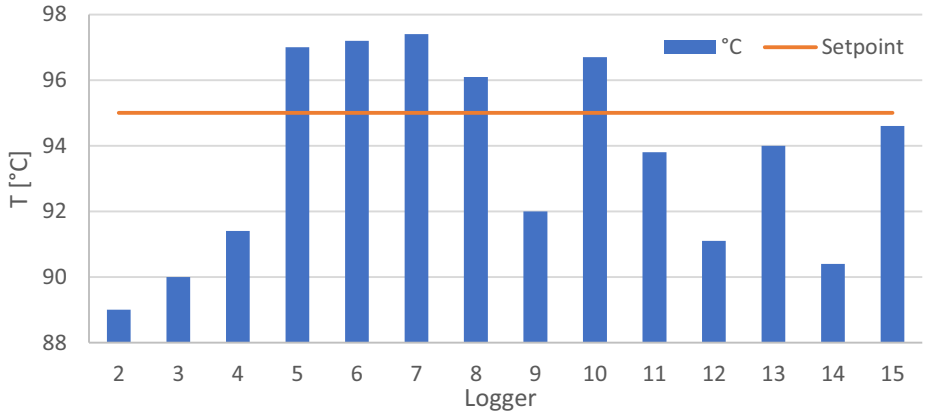

Fig. 10. Temperature distribution after 40 minutes (test 16).

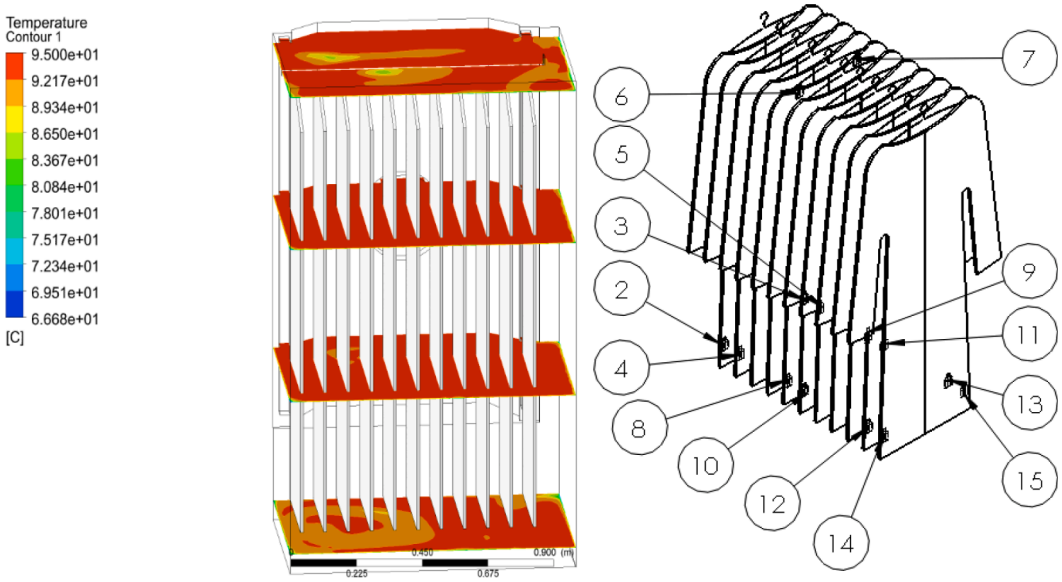

Fig. 11. CFD simulation results and data loggers positioning on the white coats.

designed thermal cycle on the white coats placed inside the chamber. In particular:

- Test 14 was used to validate a potentially candidate thermal treatment on white coats: it achieved good performances both in terms of average temperature and gradient in the chamber. The white coats heated during the test were used to realize the specimens for the subsequent mechanical tests described in the next section. Replicas of test 14, involving infected carriers, were used for microbiological test sessions 1 (30 min) and 2 (60 min).
- Test 15 emulated test 14 with dry heat. As expected, performances were poorer and thus the company reinforced the requirement of steam as heat transfer medium.
- Tests 16 and 17 aimed at validating the thermal features of the machine under 95 °C as set point, which was then required for microbiological tests of sessions 3 (60 min) and 4 (120 min). The white coats heated during test 17 were used to realize the specimens for mechanical tests.

One of the results of test 16, namely the temperature gradient in the chamber, particularly useful to validate the CFD model is worth of attention. More in detail, once the steady state conditions in the chamber were reached, after approximately 40 min, the related temperature distribution was measured by the data loggers and reported in Fig. 10.

It can be observed that loggers 2, 3, and 4 reported lower temperatures, in accordance with Fig. 11, which shows the CFD-computed temperature distribution and logger placement in the chamber. Loggers 5, 6 and 7 recorded higher temperatures again this time in line with the simulation and also with the previous results, being placed in bands A and B; loggers 13, 14, and 15, instead, are affected by the presence of the front door and placement in band C.

The comparison boundaries between the CFD simulation and the real temperature measurement in the chamber should be highlighted: specifically, the CFD simulation is simplified and does not consider the heat exchange in the heater, thus the temperature of the air inlet in the chamber is fixed and set at 95 °C, regardless of the temperature of the air outlet entering heater and its effective instant power. The machine, on the other hand, is equipped with a closed loop controller and thus heater power is adjusted accordingly. For these reasons, CFD simulation results are relevant in terms of temperature distribution and gradient, not in terms of "absolute" temperature. A measured maximum temperature of 97.4 °C and a variance of 8.1 °C is in line with the simulation.

Fig. 12. Cutting of the fabrics (left) and resulting sample (right); the pen signs represent the two segments.

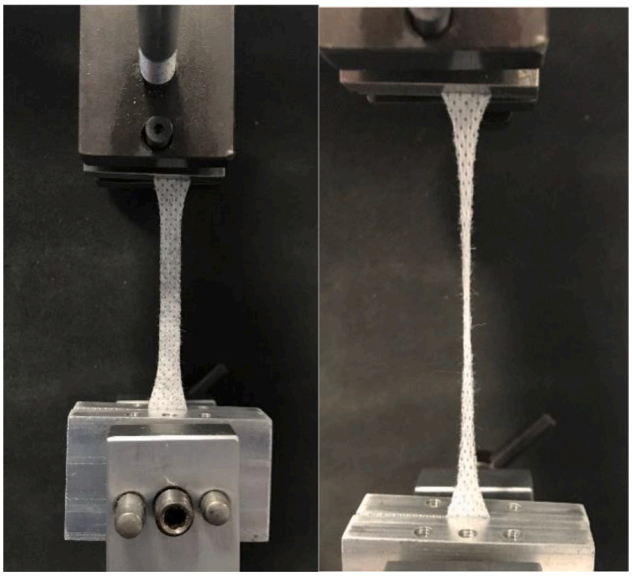

Fig. 13. Dynamometer application.

3.2. Physical and microbiological tests on PPE

Tensile tests were carried out on the disposable polypropylene white coats (0.15 mm thickness), treated according to the same thermal cycles of tests 14 and 17 to estimate the trend and the variance of the mechanical properties at different thermal cycles. Each sample (untreated white coats as reference, white coats treated at 85 °C for 1 h and white coats treated at 95 °C for 2 h, named respectively UPPE, 85PPE and 95PPE) was tested on a basis of at least six replicates.

Many efforts were made to perform valid mechanical tests and measurements, in particular:

- samples were obtained from white coats of the same model, brand and production lot, in order to guarantee, as far as possible, the same characteristics (thickness, shape, composition).
- samples were taken from the same sample area, in order to avoid anisotropic behaviour and discontinuities of the polymeric non-woven fabrics of which PPE are composed.
- samples were taken from undamaged or bent areas of the PPE. The treated devices were cut after treatment to ensure that the specimens had no heat-damaged parts. Two specimens were cut from squares samples taken from the white coats.

The cutting of the fabrics to obtain the samples was carried out as shown in Fig. 12 on the left: the material was clamped on a flat surface and a rigid sample, having standard dimensions according to the UNI EN ISO 527-2 standard, was used as a jig to obtain the test samples.

Once all the specimens were obtained from the PPE, they were then numbered and the following mean values were collected: the initial length subjected to traction (L_0), corresponding to the initial gripping distance between the dynamometer clamps, the width (W_0) and the thickness (T_0) of each sample.

Once the specimens had been cut out from treated and untreated PPE, they were samples were then fixed between the clamps of a dynamometer and analysed (Fig. 13).

Using the specific software provided by the machine manufacturer, the tensile behaviour of the material was evaluated by setting a fixed elongation speed of 5 mm/min. Force (F – [N])-Elongation (ΔL – [mm]) graph was plotted on the computer screen using the measurements recorded by the dynamometer at almost infinitesimal intervals. The F-ΔL experimental data were transformed into Stress (σ - [N/m^2])-Strain (ε - [mm/mm]) by dividing the applied force by the area of the resistant section (W_0xT_0) and the elongation by the initial useful length L_0 of the specimen. The experimentally obtained σ-ε curve is typical of toughness materials without a yield point, as displayed in Fig. 14.

Given the non-homogeneous distribution of the stress values, the experimental data (the first thousand points) were fitted by a third-degree polynomial curve (Fig. 15) and the equation obtained was used

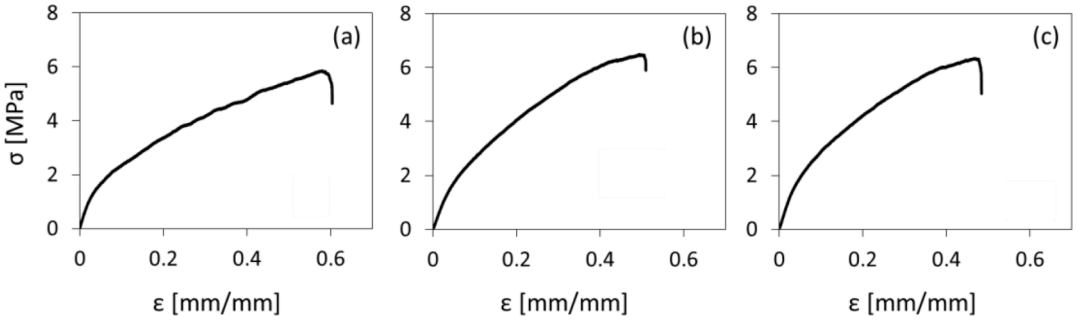

Fig. 14. Typical stress-strain curves for UPPE as reference (a), 85PPE (b) and 95PPE (c).

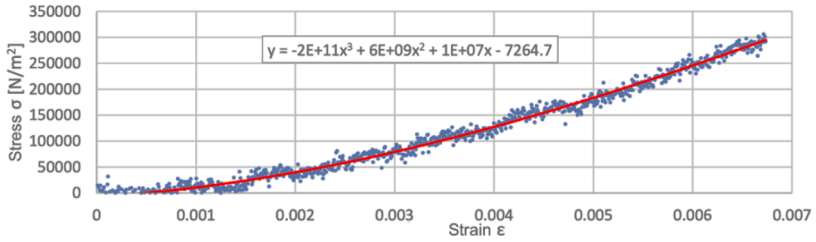

Fig. 15. Initial part of the stress-strain curve (experimental blue dots and red fitting line) for the calculation of Young's modulus.

Table 2
Mechanical parameters for UPPE, 85PPE and 95PPE.

	E [MPa]	σ_U [MPa]	ε_B [mm/mm]	T [MJoule/m^3]
UPPE	52±5	5.6±1.1	0.6±0.2	2.4±0.8
85PPE	52±5	6.3±1.3	0.5±0.1	2.2±0.9
95PPE	47±6	6.2±0.7	0.4±0.1	2.0±0.6

to calculate the σ_1 and σ_2 values, which represent the stress measured at the strain value of $\varepsilon_1 = 0.0005$ and $\varepsilon_2 = 0.0025$, respectively. Young modulus, E, was acquired by the relation $E = \frac{\sigma_2 - \sigma_1}{\varepsilon_2 - \varepsilon_1}$, according to the standard UNI ISO 527. The ultimate tensile strength, σ_U, was calculated as the maximum load supported by the specimen during the tensile test before failure. The strain at break, ε_B, was calculated as the tensile strain at the point corresponding to σ_U. For the calculation of toughness, T, the highest sums method was used: let $\sigma(\varepsilon)$ be the stress value at a given strain value in the stress-strain diagram for each interval between ε_i and ε_{i+1}, the area of the rectangle having height $\sigma(\varepsilon_{i+1})$ was calculated as $A_i = \sigma(\varepsilon_{i+1}) \cdot (\varepsilon_{i+1} - \varepsilon_i)$, and the areas of the rectangles were added up to the breakage, so $T = \sum_{\varepsilon=0}^{\varepsilon=\varepsilon_B} A_i$.

The average results and the corresponding standard deviations of the mechanical tensile tests on white coats (untreated as reference, thermal treated at 85 °C for 1 h and thermal treated at 95 °C for 2 h) are shown in Table 2 and graphically represented in Fig. 16.

The macroscopic characteristics of the white coats (colour, shape, appearance, aesthetic conditions) did not change after the heat treatments and the mechanical characteristics did not show significant differences after the treatment at 85 and 95 °C: E and σ_U remained substantially constant, while ε_B and T showed a decreasing but not significant trend because the mean values fall within the experimental standard deviation. Therefore, obtained results showed that the heat treatment allowed to keep the PPE mechanical properties unaltered, at least for one cycle, and could be considered a valid approach to guarantee their reuse safely.

Therefore, although too many re-uses of PPEs after sanitisation are not recommended given the inevitable material deterioration due to natural aging and oxidation, it is important to underline that even one or two cycles of re-use would drastically reduce the PPE request (even one reuse would halve the consumption), thus potentially mitigating the problems illustrated in the introductory section.

Microbiological tests were performed on PPE by Eurofins BioLab (Milan, Italy). A bovine coronavirus, BCoV RVB-0020, was used to perform an efficacy test of the projected sanitisation system according to UNI EN 16777:2018 and UNI EN 16777:2019 standards. BCoV was already used as a surrogate for SARS-related viruses (including Sars-CoV-2) as it belongs to the same *Betacoronavirus* genus, having a similar morphology and size, but at a Bio Safety Level 2 [12,13].

Samples were taken from the same white coats and masks used in the previous tests, by cutting approximately 2.5 × 4 cm^2. After a preliminarily sterilisation, these carriers were inoculated with BCoV by immersion for 15 min in 10 ml of viral suspension, then placed on Petri plates and let dry under the air flow of the biohazard hood.

Two carriers of each PPE were used as a control (non-treated) samples, through an immediate recovery in 2 ml of Universal Transport Medium (UTM®, Copan, Murrieta, USA) supplemented with 2% foetal bovine serum (Gibco, Invitrogen, CA, USA); the remaining were placed in closed sterile cups and refrigerated until tests were performed.

For the thermal treatments, 5 inoculated carriers obtained from the white coats were hooked inside a sterile white coat, in different positions. Furthermore, the 2 carriers obtained from face masks were placed

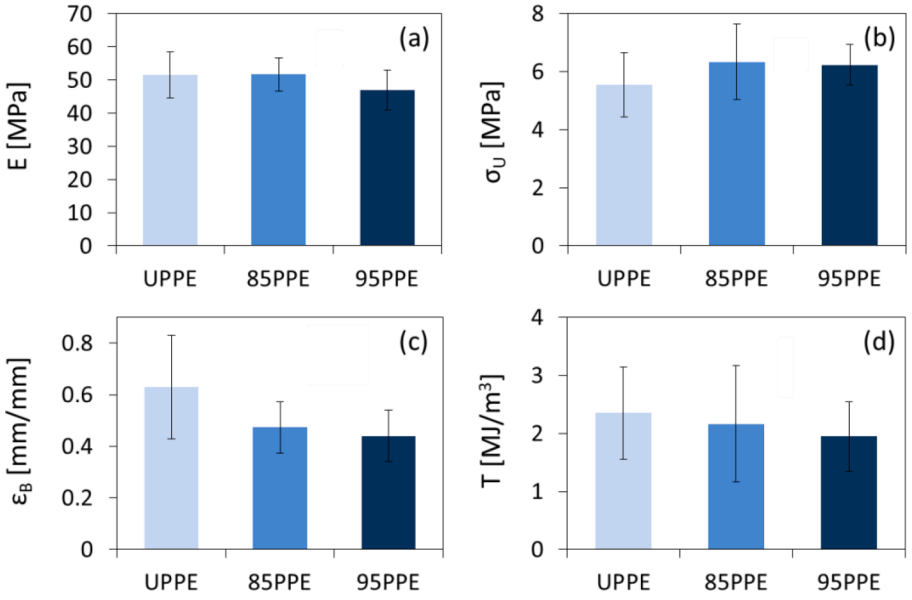

Fig. 16. Variations of the tensile properties for UPPE, 85PPE and 95PPE: E (a), σ_U (b), ε_B (c) and T (d).

Table 3
Experimental conditions of the four test sessions.

Test session	Temperature Set Point [°C]	Limit temperature [°C]	Cycle duration [min]
1	85	95	30
2	85	95	60
3	95	105	60
4	95	105	120

on a sterile mask, one inside and one outside.

The white coat and the mask with the inoculated carriers were placed on special hangers, then positioned on the appropriate support inside the machine. To get a representative view of the least-favoured positions, they were put between the 5th and 6th coats out of the 11 that the machine can host.

Four different sessions were carried out, with parameters resumed in Table 3.

After each treatment, carriers were recovered with sterile tweezers and placed inside tubes with 2 ml of maintenance medium.

Two further untreated carriers for each PPE were recovered in 2 ml of maintenance medium and used for validation of viral recovery at the end of the time required for carrying out the tests.

All tubes were immediately refrigerated, transported to the laboratory, and analysed upon arrival. Tubes were vortexed for 1 min, serially diluted and 0.1 ml of each dilution was placed into 6 of 96 wells microplates containing the cellular confluent monolayer.

At the end of the required incubation period, the cellular culture was observed with inverted microscope to detect any cytopathic effect (CPE) due to viral suspension. After this detection the infecting activity (TCID50 evaluation) was calculated by means of the Spearman – Kärber method [14]. The reduction of virus titre was calculated from titre differences between carriers thermally treated and control carriers (untreated).

The results of microbiological analysis are reported in Table 4.

4. Discussion

Starting from the microbiological results, they showed that a viral load reduction could be obtained by a sterilisation process made using a machine originally conceived as a food oven and reengineered for decontamination purposes. However, on the samples under investigation, at least 95 °C and a 1 h cycle were required to completely inactivate the BCoV virus. Despite the tests were conducted on a surrogate of the Sars-CoV-2, it could be assumed that the designed treatment could be effective also in sterilizing Sars-CoV-2 contaminated samples as several documents proved that treatments applied to surrogate viruses (such as BCoV, H1N1, H5N1 or Sars-CoV) could be successfully applied with the Sars-CoV-2 virus as well [15–17,5].

On the other hand, our result showed that a more intensive treatment is required to completely inactivate the virus, compared to the outcomes available in literature, which report the complete inactivation of similar viruses with milder treatments (60 °C and 1 h cycle, e.g., [18]). Table 5 resumes the PPE/material tested, temperature and duration of the thermal treatment, heat type and virus under examination in the papers used as reference.

According to the reported duration and temperature of treatments, assuming that a reduction of infectivity greater than 5.0 $\log_{10}$ involves the complete inactivation of the virus (green colour), between 3 and 5 $\log_{10}$ corresponds to an average abatement (yellow colour), while inferior to 3 $\log_{10}$ to a scarce abatement (red colour), Fig. 17 was built for visually summarizing the performances of the treatments reported in

Table 4
Results from the thermal treatments of the 4 test sessions, including initial conditions details.

Test session	Pre-treatment virus titre (Log $TCID_{50}$)	White Coats			Face Masks			Notes at the end of the disinfection cycle
		Titre on coat Log $TCID_{50}$	Log reductions	% reduction	Titre on mask Log $TCID_{50}$	Log reductions	% reduction	
1	6.67	5.72	2.42 ± 0.11	99.62%	5.39	3.67 ± 0.108	99.98%	Residual virus was detected on the carriers.
2	6.67	5.72	4.02 ± 0.12	99.99%	5.39	4.17 ± 0.04	99.99%	
3	6.00	4.89	≥ 4.59 ± 0.09	> 99.99%	5.38	≥ 5 ± 0	> 99.99%	No residual virus was detected on the carriers.
4	6.00	4.89	≥ 4.59 ± 0.09	> 99.99%	5.38	≥ 5 ± 0	> 99.99%	

Table 5
Characteristics found in previous studies of PPE thermal sanitisation.

PPE/material tested	Temperature [°C]	Duration [min]	Dry/Steam Heat	Result on virus	Virus	Ref.
-	75	30	Dry	Inactivated	Sars-CoV	[19]
Face mask N95	60	30	Steam	99.9% inactivated	Sars-Cov-2	[20,16]
-	70	30	Steam	Inactivated	H1N1, H5N1	[21]
Polypropylene	56	60	Dry	Not inactivated (but very close)	Sars-CoV	[22]
Polypropylene	65	60	Dry	Not inactivated (but very close)	Sars-CoV	[22]
Polypropylene	75	45	Dry	Inactivated	Sars-CoV	[22]
In tube suspensions	56	5	Dry	5.8 $\log_{10}$ reduction of viral infectivity	Sars-CoV	[23]
In tube suspensions	56	10	Dry	6.48 $\log_{10}$ reduction of viral infectivity	Sars-CoV	[23]
In tube suspensions	56	30	Dry	>6.48 $\log_{10}$ reduction of viral infectivity	Sars-CoV	[23]
In tube suspensions	30	56	Dry	1.9-5.0 $\log_{10}$ reduction of viral infectivity	Sars-CoV	[24]
In tube suspensions	60	30	Dry	≥5.0 $\log_{10}$ reduction of viral infectivity	Sars-CoV	[24]
In tube suspensions	60	30	Dry	≥4.0 $\log_{10}$ reduction of viral infectivity	Sars-CoV	[25]
In tube suspensions	60	60	Dry	≥4.0 $\log_{10}$ reduction of viral infectivity	Sars-CoV	[25]
In tube suspensions	65	10	Dry	≥4.3 $\log_{10}$ reduction of viral infectivity	Sars-CoV	[26]
In tube suspensions	65	15	Dry	≥4.3 $\log_{10}$ reduction of viral infectivity	Sars-CoV	[26]
Face mask N95	70	60	Dry	Inactivated	Sars-Cov-2	[27]
Surgical and N95 face mask	60	60	Dry	Inactivated	Sars-Cov-2	[28]

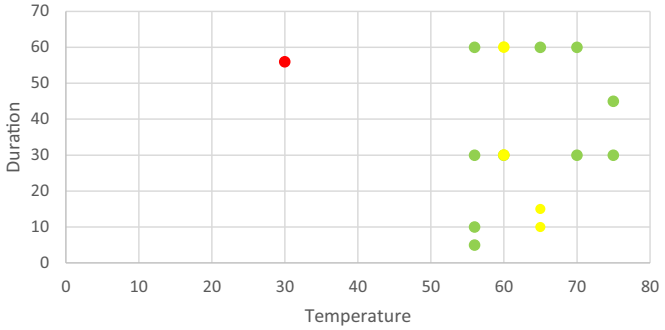

Fig. 17. Virus abatement according to duration of the treatment and temperature; Temperature [°C] and Duration [min].

the literature.

According to Fig. 17, the best outcomes in terms of virus reduction would be obtained starting from 56 °C for very short cycles (5–10 min); however, if the specific virus Sars-CoV-2 is considered, total inactivation would be reached in dry conditions starting from a temperature of 60 °C and 60 min treatment [21,28]. Moreover, the considered studies were mainly carried out in laboratory settings, while in this paper the efficacy of the thermal treatment was tested on specific PPE (white coats and masks) and could be thus useful for determining the settings of sterilisation cycles in real cases.

Despite we did not take into account the filtration performance of the treated PPE, previous studies demonstrated that when performing thermal treatments on facial masks for no more than 24 h at 80–95 °C (so greater duration and temperature of the presently reported values), no significant negative impacts on filtering capacity were observed [28].

5. Conclusions

Given the recent challenges brought by the COVID-19 pandemic caused by the Sars-CoV-2 virus, among which that of PPE stands out, this research aimed at proposing an innovative machine for sanitisation of these tools and a reduction of biological risk. The evidence of the effects of thermal treatments on Coronavirus contaminated specific material (non-woven) is provided, and the different design and development phases of the machinery are illustrated, including some solutions to technical issues which may occur.

As the machinery has been developed from a pre-existing oven built for food purposes, a limited number of interventions have been necessary. In fact, by nature, it is already designed and built according to hygienic criteria, it can reach proper temperatures and its size is adequate for hosting, for instance, white coats.

According to several tests carried out, the projected treatment was able to completely inactivate a BovC virus at 95 °C for 1 h.

As far as the PPE mechanical properties are considered, according to the illustrated results, one cycle can be scientifically guaranteed; further investigations are required to determine whether this value can be increased or not, depending on the mechanical behaviour. However, it is important to emphasise that even one or two re-uses would drastically reduce demand of PPE, with economic and environmental advantages and risk reduction (which could derive from multiple usages).

Few studies in the literature have dealt with the effects of thermal treatments on Sars-CoV-2 virus and most of the existing papers refer to face masks, while not considering white coats; this study contributes to closing this gap. Finally, no solutions able of being industrialised have been developed and proposed so far for these purposes. The developed machine represents a completely new and innovative solution, intended to be industrialised and commercialised in the future. For supporting that, it is in plan to implement the solution in a company committed to provide the mandatory PPE for their workers for safety purposes, and an assessment in quantitative terms will be performed (both on PPE saved in a determined time span, and accordingly on the economic aspect). Moreover, broadening applications, since the machine was derived from an industrial food oven, higher temperatures can be easily reached unlocking the set-point to use it also for sanitizing other thermal-resistant PPE with respect also to other viruses, thus increasing the fields of application.

References

[1] E.V. Sargent, F. Gallo, Use of Personal Protective Equipment for respiratory protection, ILAR J. 44 (1) (2003) 52–56.
[2] S. Kasloff, A. Leung, J. Strong, D. Funk, T. Cutts, "Stability of Sars-CoV-2 on crtitical Personal Protective Equipment, Sci. Rep. 11 (2021) 984.
[3] World Health Organization, 2020. [Online]. Available: www.who.int/news-room/detail/03-03-2020-shortage-of-personal-protec-tive-equipment-endangeringhealth-workers-worldwide (Accessed on May 2021).
[4] A. Cramer, E. Tian, S. Yu, M. Galanek, E. Lamere, J. Li, R. Gupta, M. Philip Short, "Disposable N95 masks pass qualitative fit-test but have decreased filtration efficiency after cobalt-60 gamma irradiation," Pre-Print, 2020.
[5] D. Weaver, B. McElvany, V. Gopalakrishnan, K. Card, D. Crozier, A. Dhawan, M. Dinh, E. Dolson, N. Farrokhian, M. Hitomi, E. Ho, T. Jagdish, E. King, J. Cadnum, C. Donskey, N. Krishnan, G. Kuzmin, J. Li, J. Maltas, J. Mo, "UV decontamination of Personal Protective Equipment with idle laboratory biosafety cabinets during the COVID-19 pandemic, PLoS One 16 (7) (2021), e0241734.
[6] M. Bergman, D. Viscusi, B. Heimbuch, J. Wander, A. Sambol, R. Shaffer, "Evaluation of multiple (3- Cycle) decontamination processing for filtering facepiece respirators, J. Eng. Fiber Fabr. 5 (4) (2010) 33–41.
[7] B. Columbus, "Final report for the bioquell hydrogen peroxide vapor (HPV) decontamination for reuse of N95 respirators," 2016. [Online]. Available: https://www.fda.gov/media/136386/download.
[8] A. Kumar, S. Kasloff, A. Leung, T. Cutts Id, J. Strongid, K. Hills, F. Gu, P. Chen, G. Vazquez-Grande, B. Rush, S. Lother, K. Malo, R. Zarychanski, J. Krishnan, "Decontamination of N95 masks for re-use employing 7 widely available sterilization methods well-resourced settings, the application of moist heat may allow local processing of N95 masks, PLoS One 15 (12) (2020).
[9] E. Grignani, A. Mansi, R. Cabella, P. Castellano, A. Tirabasso, R. Sisto, M. Spagnoli, G. Fabrizi, F. Frigerio, G. Tranfo, Safe and effective use of ozone as air and surface disinfectant in the conjuncture of COVID-19, Gases 1 (2021) 19–32.
[10] L. Liao, W. Xiao, M. Zhao, X. Yu, H. Wang, Q. Wang, S. Chu, Y. Cui, "Can N95 respirators be reused after disinfection? How many times? ACS Nano 14 (5) (2020) 6348–6356.
[11] E. Bottani, R. Montanari, A. Volpi, G. Di Maria, F. Solari, L. Tebaldi, "Converting a food oven into a thermal sanitizer for Personal Protective Equipment against COVID-19: computational fluid dynamics simulation, in: Proceedings of the 7th International Food Operations & Processing Simulation Workshop of the 18th International Multidisciplinary Modeling & Simulation Multiconference, Virtual Conference, 2021.
[12] B. Lau, D. Becher, M. Hessling, High intensity violet light (405 nm) inactivates coronaviruses in phosphate buffered saline (PBS) and on surfaces, Photonics 8 (414) (2021).
[13] J.J. Wensman, M. Stokstad, Could naturally occurring coronaviral diseases in animals serve as models for COVID-19? A review focusing on the bovine model, Pathogens 9 (991) (2020).
[14] M. Ramakrishnan, "Determination of 50% endpoint titer using a simple formula, World J. Virol. 5 (2) (2016) 85–86.
[15] World Healt Organization, First Data on Stability and Resistance of SARS Coronavirus compiled by Members of WHO Laboratory Network, World Healt Organization, 2020 [Online]. Available, https://www.who.int/csr/sars/survival_2003_05_04/en/ (Accessed on May 2021).
[16] United States Environmental Protection Agency, "About List N: Disinfectants for Coronavirus (COVID-19)," 2020. [Online]. Available: https://www.epa.gov/coronavirus/about-list-n-disinfectants-coronavirus-covi-19-0 (Accessed on May 2021).
[17] A. Chin, J. Chu, M. Perera, K. Hui, H.L. Yen, M. Chan, M. Peiris, L. Poon, "Stability of SARS-CoV-2 in different environment conditions," Correspondence, vol. 1, n. 1, p. E10, 2020.
[18] L. Guillier, S. Martin-Latil, E. Chaix, A. Thébault, N. Pavio, S. Le Poder, C. Batéjat, F. Biot, L. Koch, D. Schaffner, M. Sanaa, Covid-19 Emergency Collective Expert Appraisal Group, "Modeling the inactivation of viruses from the coronaviridae family in response to temperature and relative humidity in suspensions or on surfaces, Appl. Environ. Microbiol. 86 (18) (2020) e01220–e01244.
[19] S.M. Duan, X.S. Zhao, R.F. Wen, J.J. Huang, G.H. Pi, S.X. Zhang, J. Han, S.L. Bi, L. Ruan, X.P. Dong, SARS Reserach Team, Stability of SARS coronavirus in human specimens and environment and its sensitivity to heating and UV irradiation, Biomed. Environ. Sci. 16 (2003) 246–255.
[20] Centers for Disease Control and Prevention, "Implementing filtering facepiece respirator (FFR) reuse, including reuse after decontamination, when there are known shortages of N95 respirators," 2020. [Online]. Available: https://www.cdc.gov/coronavirus/2019-ncov/hcp/ppe-strategy/decontamination-reuse-respirators.html. (Accessed on May 2021).
[21] C. Celina, E. Martinez, M. Omana, A. Sanchez, D. Wiemann, M. Tezak, T. Dargaville, Extended use of face masks during the COVID-19 pandemic - thermal conditioning and spray-on surface disinfection, Polym. Degrad. Stab. 179 (2020), 109251.

[22] M. Darnell, K. Subbarao, S. Feinstone, D. Taylor, "Inactivation of the coronavirus that induces severe acute respiratory syndrome, SARS-CoV, J. Virol. Methods 121 (1) (2004) 85–91.
[23] H. Kariwa, N. Fujii, I. Takashima, Inactivation of SARS coronavirus by means of povidone-iodine, physical conditions, and chemical reagents, Jpn. J. Vet. Res. 52 (2004) 105–112.
[24] H. Rabenau, J. Cinatl, B. Morgensten, G. Bauer, W. Preiser, H. Doerr, Stability and inactivation of SARS coronavirus, Med. Microbiol. Immunol. 194 (2005) 1–6.
[25] M. Yunoki, T. Urayama, I. Yamamoto, S. Abe, K. Ikuta, "Heat sensitivity of a SARS-associated coronavirus introduced into plasma products, Vox Sang. 87 (2004) 302–303.
[26] M. Darnell, D. Taylor, "Evaluation of inactivations methods for severe acute respiratory syndrome coronavirus in noncellular blood products, Transfusion 46 (2006) 1770–1777.
[27] P. Juang, P. Tsai, "N95 respirator cleaning and reuse methods proposed by the inventor of the N95 mask material, J. Emerg. Med. 58 (5) (2020) 817–820.
[28] Y. Xiang, Q. Song, W. Gu, Decontamination of surgical face masks and N95 respirators by dry heat pasteurization for one hour at 70°C, Am. J. Infect. Control 48 (8) (2020) 880–882.